

# Magnet Design of a Prototype Structure for the X-ray FELs at TESLA

M. Tischer, J. Pflüger

*Hamburger Synchrotronstrahlungslabor HASYLAB, DESY, Notkestr. 85, D-22603 Hamburg, Germany*

## Abstract

XFEL undulators for the TESLA project require high quality in order to drive the SASE process into saturation. On the other hand, as large quantities are needed for the five SASE undulators, it is rather important not to oversize the undulator design. The magnet structure is the most delicate and most expensive part of an insertion device. This report proposes a magnet design for a SASE undulator with tunable wavelength in the 1 Å regime. The layout of the magnet structure is optimized for a 60 mm undulator period which requires a magnet volume of 400 cm<sup>3</sup> per period to gain a peak field of 1.33 T. An end pole configuration of the gap variable device is suggested so that both field integrals are trimmed close to zero for all gaps.

## 1 Introduction

Five SASE FELs and five spontaneous undulator systems are planned for the TESLA FEL project. The overall concept of the FEL laboratory is defined in the TESLA Technical Design Report (TDR) [1], a general layout of the undulator systems can be found in Section 5 therein. Four of the five SASE FELs will be planar devices covering a wavelength range from 0.85 Å to 5.0 Å. The SASE5 will be a helical undulator in the 4–58 Å region while the majority of the spontaneous undulators will operate in the hard X-ray regime.

These X-ray SASE FELs require a tremendous length of each undulator system exceeding 200 m. Therefore, an undulator system will be subdivided into 6.1 m long cells. A large beta function allows to separate the focussing section for the electron beam from the magnetic undulator structure (in contrast to e.g. the FEL at the TESLA Test Facility) and thus, enormously facilitates the magnet design and survey, and also the installation. Each undulator cell consists of a gap variable undulator segment of 5 m length and an intersection module containing various items such as a phase shifter, a quadrupole with integrated BPM, steering coils, and vacuum components. Gap motion and gap dependent settings of phase shifter, steerers, etc. will be managed within each cell by a local control system which is part of a central undulator control unit.

In total, about 280 undulator cells are required for the ten undulator systems at TESLA. This calls for design unification and standardization wherever it is possible. In case of the magnet structures only four different types will be necessary to achieve the various radiation properties of the ten undulators: For the planar systems 106 segments with  $\lambda_u = 60$  mm, 96 with  $\lambda_u = 45$  mm, 50 with  $\lambda_u = 30$  mm for the spontaneous devices, and finally 29 segments for the helical undulator. Except for the latter, also their mechanical structure will be very similar. Heavy prototyping of all components is required well in advance to the later production phase which will be manufactured on industrial scale as turnkey ready devices.

The overall concept of the TESLA undulator systems is presented in the TDR [1] while specific design and prototyping issues of the different components have been broken down and addressed in separate reports dealing on the mechanical structure [2], the control system [3], the phase shifter [4], field accuracy requirements [5], the electron beam focussing optics [6], a concept for the helical undulator [7], and on large scale production strategies [8]. The present report discusses a prototype magnet structure for SASE1/4 with  $\lambda_u = 60$  mm, representative for all planar undulator systems. Optimization of the geometrical properties is investigated with respect to the required field accuracy, and a possible end pole configuration for a balanced and gap independent first field integral is proposed.

Any change of initial field specifications towards a smaller minimum gap, a more ample reserve in peak field or transverse good-field-region has a considerable impact on the total costs. For example, providing an additional magnet width of 1 cm together with ~5 mm wider poles, results in an improvement of the transverse field plateau by only ~40%, however,

causes extra costs of about 2.2 Mio € for all TESLA undulators as a whole. Hence, arbitrary oversize of especially the magnet structure should be avoided.

## 2 Field Requirements

A variety of different technologies has been proposed in the past to build insertion devices. A comprehensive review and comparison is given by Refs. [9] and [10]. Permanent magnet devices are the most promising choice since this technology is most appropriate for the proposed X-FEL undulators and is developed furthest. Both fundamental designs had been proposed by Halbach [11], i.e. pure permanent magnet (PPM) undulators and hybrid devices using iron poles which are excited by adjacent permanent magnets (PM). While properties of the magnet material itself are limiting the field quality of PPM devices, the pole geometry strongly determines the magnetic properties of a hybrid undulator and field quality especially depends on the precision of the machined pole faces. Hybrid structures which generally achieve higher peak fields will be used for all TESLA X-FEL undulators except for SASE5 which will produce circularly polarized light by means of a modified planar PPM structure [7].

The Pierce parameter  $\rho$  is a fundamental quantity in FEL theory determining properties like spectral bandwidth or power growth rate. Thus, it also gives a natural measure for some accuracy requirements of the undulator magnetic field. The  $\rho$ -parameter is about  $4 \cdot 10^{-4}$  in the short wavelength regime of SASE1/4.

- i) The field roll-off, i.e. the transverse homogeneity of the vertical magnetic field  $\Delta B_z(x)/B_z(x=0)$ , has to be  $< \rho$  over a sufficiently broad region. Though the electron beam itself has an rms-width of only  $\sim 35 \mu\text{m}$ , a transverse good-field-region with a width of  $\pm 1 \text{ mm}$  for  $12 \text{ mm} \leq \text{gap} \leq 24 \text{ mm}$  is desired to cover tolerances and to keep the horizontal alignment effort of the undulator segments moderate.
- ii) The FEL process is very sensitive to any deterioration of the overlap of electron beam and radiation field. The main contribution to that arises from random trajectory offsets at the quadrupole locations. A random quadrupole offset of  $1 \mu\text{m}$  will lead to a gain reduction of  $\sim 10\%$  [5]. According to that, an orbit displacement by  $1 \mu\text{m}$ , corresponding to a 2<sup>nd</sup> field integral of  $I_2 = 83 \text{ Tmm}^2$ , is considered as upper limit for the residual value within a single undulator segment.
- iii) Analogous to the displacement requirements, the angular trajectory misalignment within a single cell has to be smaller than  $0.2 \mu\text{rad}$ .

- iv) The peak field enhancement scales linearly with the reduction in saturation length [10]. Therefore, the minimum gap should be as small as possible. However, it is known that too small apertures deteriorate electron bunches with huge charge density due to wake fields which the head induces to the tail of a bunch. Different models and assumptions are reported in the literature [12] in order to predict wake field effects. Referring to the present status of this discussion a minimum magnetic gap of 12 mm is considered as a design constraint [1].

From the specified radiation wavelength range together with the minimum gap of 12 mm and a maximum peak field  $B_0 = 1.33$  T the optimum undulator period length of SASE1/4 has been calculated to  $\lambda_U = 60$  mm. While the gap consideration (iv) is a more general restriction to be taken into account the other conditions are specific design issues which have to be optimized for each magnet structure type individually; the appropriate transverse field plateau (i) is a property of the main magnet structure, whereas balanced field integrals (ii - iii) have to be assured by suitable end poles.

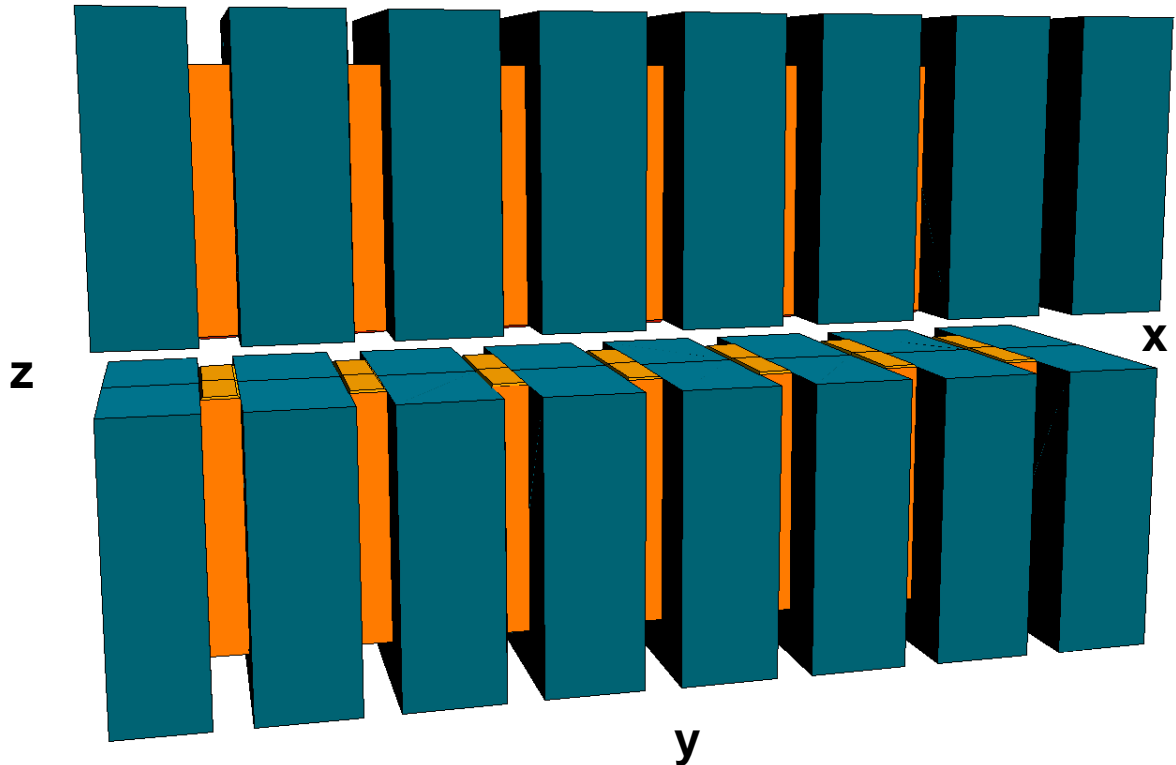


**Fig. 1:** Part of the PM hybrid structure of SASE1/4 resembling the final proportions of magnets and poles.

### 3 Hybrid Structure Design

The properties of a magnet structure depend on a variety of different parameters which interact to a considerable degree. Optimization is, hence, an iterative process. The goal of this study is to find a concept matching all criteria discussed above with a minimum of magnet material, which is the most expensive part of an undulator system. Due to the large number of devices any optimization of the magnet design has big impact on the total costs and, hence, proportions of poles and magnets have to exploit the magnet material as much as possible. The magnet design has been calculated using the Radia code [13]. Only a representative sub-unit with several periods of a complete wiggler segment has been computed for determination of the magnetic properties. Sufficient segmentation of the single elements of the magnet structure was proven in order to assure convergence and reliable results of the calculation.

In a gap variable undulator both field integrals have to be trimmed to zero by means of a special end pole configuration. Therefore, a symmetric field configuration is chosen so that the 2<sup>nd</sup> field integral cancels once the 1<sup>st</sup> field integral is tuned to zero. The magnet structure consists of a conventional hybrid structure using NdFeB magnets with a remanent magnetization  $M_r = 1.15$  T. Poles are made of a material with high permeability like Vanadium Permendur or Vacoflux to lower saturation effects in the poles. With respect to the magnets, the pole tips have a small overhang of 0.5 mm into the gap region to avoid saturation effects at the corners and a chamfer of the same amount which approximates a removal of sharp edges. The transverse and vertical magnet overhang as well as all other geometrical dimensions of magnets and poles are parameters in the calculation which will be determined in the following. Fig. 1 shows the proportions of the magnet structure in the final design.

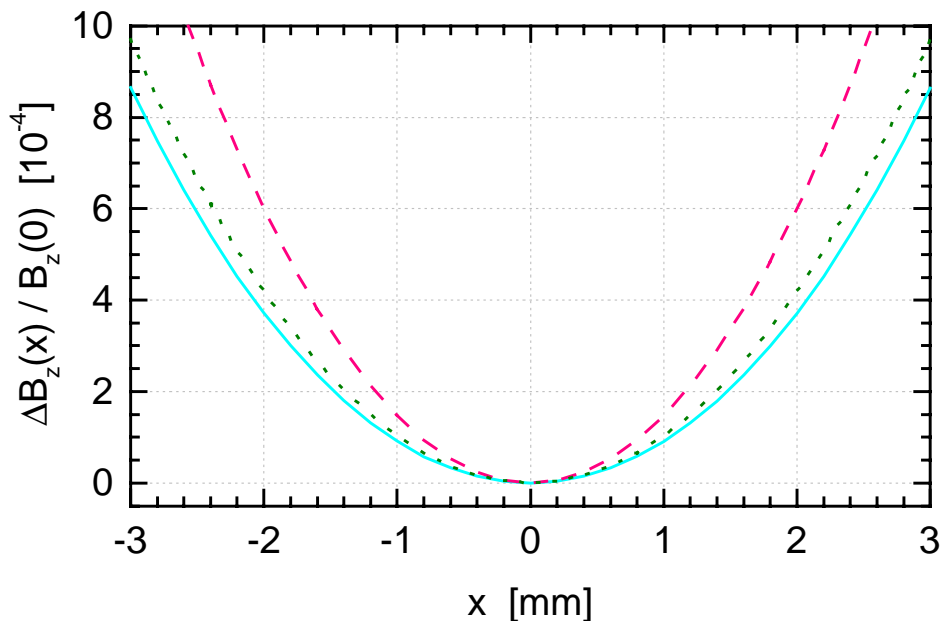


**Fig. 2:** Peak field stability in transverse direction for various parameter sets of gap / pole length : — 12 mm / 8 mm, - - - 24 mm / 8 mm, ···· 12 mm / 7 mm.

A large transverse good-field-region requires broad poles while a smaller pole width enhances the peak field for constant magnet parameters; similar arguments hold for the pole length. The reverse dependence on the pole width illustrates the mutual impact of several properties which have to be optimized simultaneously. Several sets of multi-parameter calculation were performed to screen the parameter space and to find the optimum geometry for the specified constraints.

The transverse peak field homogeneity  $\Delta B_z(x)/B_z(x=0)$  should be in the order of the  $\rho$ -parameter, i.e.  $4 \cdot 10^{-4}$ , within each pole over a distance range  $\pm 1$  mm. The interesting case is the open gap position which corresponds to the shortest wavelength and, therefore, needs the highest field quality. Figure 2 illustrates the transverse field roll-off and its dependence on pole length and gap. For a pole length of 8 mm a peak field deviation of  $< 2 \cdot 10^{-4}$  is obtained at 24 mm gap within  $|x| \leq 1$  mm. At 12 mm gap the field is constant within  $\sim 1 \cdot 10^{-4}$ . These values are achieved for a pole width of 40 mm.

The pole length is usually optimized versus the magnet length in terms of maximum peak field for a given undulator period  $\lambda_U$ . In our case with  $\lambda_U = 60$  mm, a maximum  $B_z$  resulted for a pole length of about 8 mm and a corresponding magnet length of 22 mm as shown in Fig. 3.

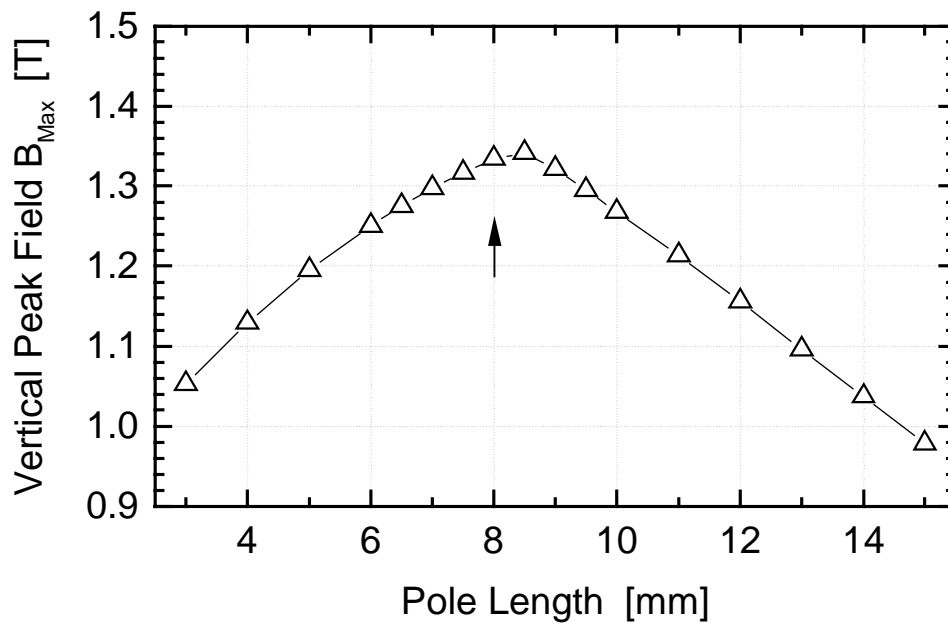


**Fig. 3:** Dependence of the vertical peak field on the pole length for constant period length; the arrow marks the design value.

For a given magnet volume the peak field dependence on pole height and the transverse proportions of the magnet is less pronounced. Figure 4 shows for different magnet length how the transverse properties act on the peak field; it should be noted that the magnet volume is kept constant in all cases. The optimum magnet cross section of  $65 \times 70$  mm<sup>2</sup> (height  $\times$  width) is related to a pole height of 55 mm and a width of 40 mm.

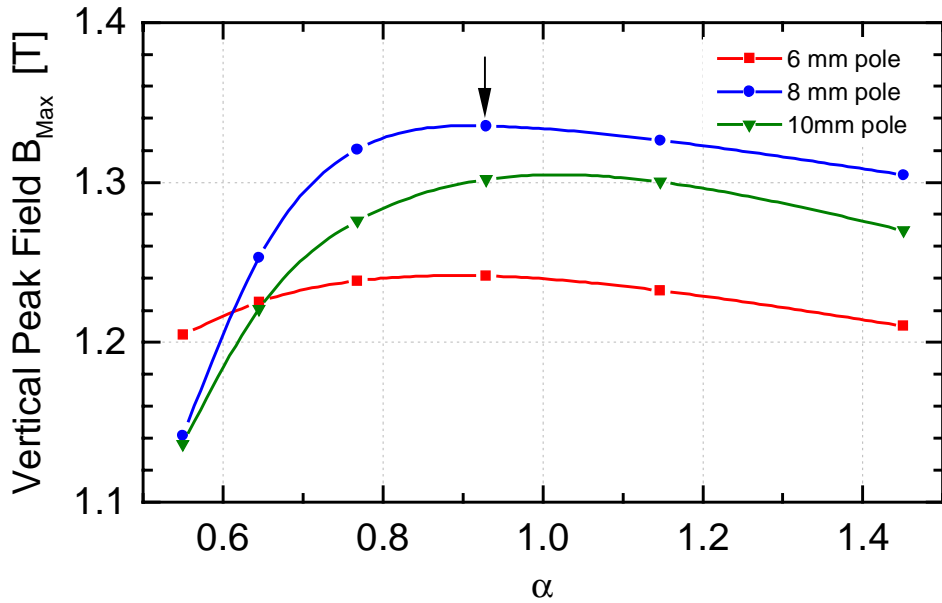


**Fig. 4:** Peak field as function of the ratio of magnet height to magnet width. The curves correspond to different pole length with the constraint of constant  $\lambda_U = 60$  mm and constant magnet volume; the arrow marks the design value.

In the above considerations on a maximum peak field  $B_z$  the magnet volume was kept at a constant value. It is obvious that the peak field can easily be enhanced by increasing the overall magnet size, however, using bigger magnets without optimizing their shape would be a waste of magnet material which is not contributing to the field generation in an optimum way. Only a simple rectangular shape of poles and magnets is regarded as a concession to the ease of manufacturing and construction. There is no sharp criterion for the most useful amount of

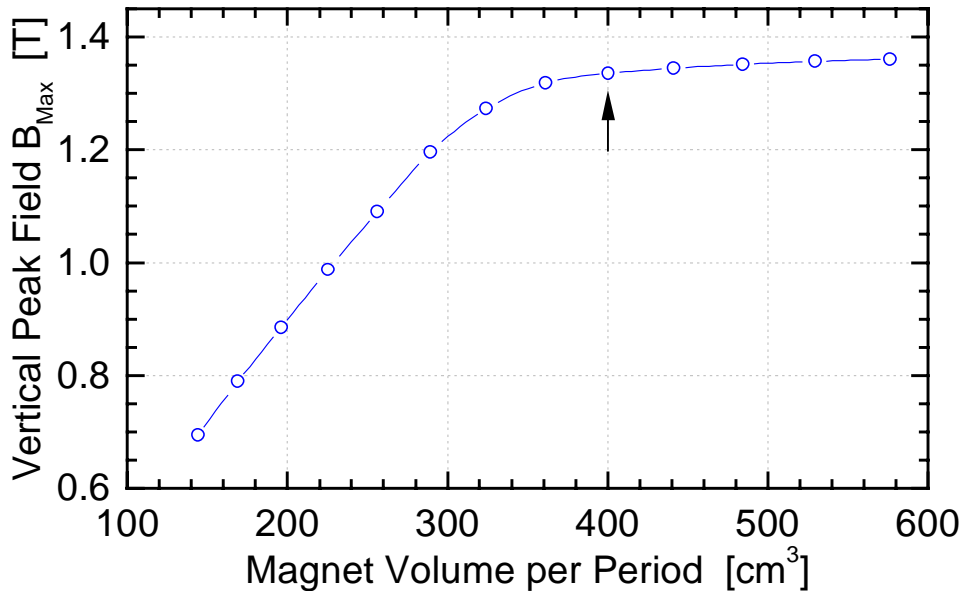


**Fig. 5:** Peak field growth as function of the applied magnet volume for constant  $\lambda_U$  and constant transverse magnet proportions; the arrow marks the design value.

magnet material. This is illustrated in Fig. 5. Due to the finite permeability of the pole material the magnetic field saturates. A magnet volume of  $400 \text{ cm}^3$  per undulator period is needed generate a magnetic field with sufficient quality and a peak value of  $B_0 = 1.33 \text{ T}$ . The rather abstract figure of merit, namely performance as function of overall costs, is difficult to factorize entirely as the system, which has to be considered as a whole (including infra-structural aspects), has many mutually interacting features. The present design value is a good compromise as the magnet volume is located near the transition to the asymptotic part of the curve.

Finally, Fig. 6 displays the gap dependence of the on-axis peak field  $B_0$ . The values for the closed and open gap position at 12 mm and 24 mm are 1.33 T and 0.577 T, respectively; the corresponding rms field values are  $B_0^{\text{rms}} = 0.84 \text{ T}$  and  $B_0^{\text{rms}} = 0.39 \text{ T}$ . This is close to the rms values of a pure sinusoidal field indicating a low content of higher harmonics. The solid curve in Fig. 6 represents a fit to the calculated data points according to

$$B_0[T] = a_1 \cdot \exp\left\{a_2 \cdot \frac{g}{\lambda_u} + a_3 \cdot \left(\frac{g}{\lambda_u}\right)^2\right\} \quad (1)$$

with the parameters  $a_1 = 3.56$ ,  $a_2 = -5.25$ , and  $a_3 = 1.67$  for  $\lambda_u = 60 \text{ mm}$ . These values, i.e. the peak fields, are slightly smaller than those reported by P. Elleaume et al. [10] since the transverse magnet dimensions are kept significantly smaller in the present design. A maximum peak field  $B_0 = 1.33 \text{ T}$  is obtained for poles made from cobalt iron alloy while in case of low carbon steel poles only 1.27 T would be achieved due to a lower saturation level in the latter.

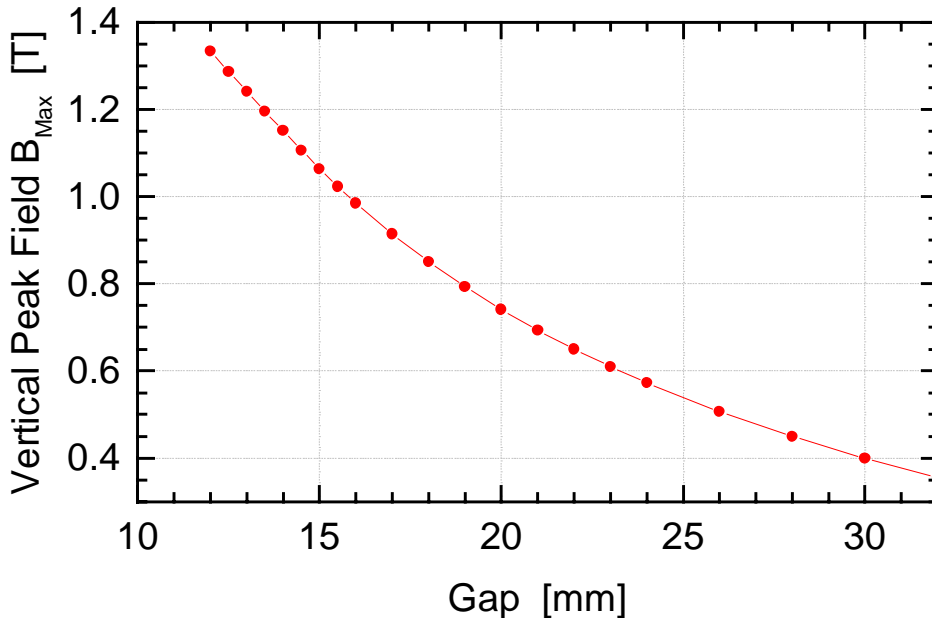


**Fig. 6:** Gap dependence of the peak field in the optimized magnet design of SASE1/4.

#### 4 End Pole Configuration

End pole configuration of multi-segmented devices is a critical issue in the magnet design. Residual field integrals should be compensated for all gaps as good as possible by appropriate passive elements. Inevitable remaining small kicks on the electron trajectory have to be compensated by shims and by small active correctors. The undulator segment is designed in a symmetric way so that the 2<sup>nd</sup> field integral cancels once the 1<sup>st</sup> field integral is tuned to zero.

Field clamps confining the magnetic flux can be used to avoid large extension of fringe fields and to reduce their gap dependence. The last magnets within one magnet structure half have reversal field orientation in a symmetrical field configuration so that a field clamp on zero magnetic potential will not close the magnetic field lines across the girder. Though the field clamp per-se confines the fringe fields in axial direction the field lines in this case will be closed across the gap; in this respect the clamp behaves like a pole and, hence, it has to be assured by a special shape of the field clamp that the magnetic flux will circumvent the beam stay clear for all gap positions. Unless this can be achieved, a field clamp in a symmetrical field configuration will result in a higher gap dependence of the field integrals. Therefore, the present prototype magnet structure disregards such a complicated field clamp.

There is a wide range of possibilities how to trim the field integral gap independently by means of special arrangement and dimension of the last poles or magnets, i.e. by means of passive elements. A widely used concept is to downsize the two final magnets and balance the 2<sup>nd</sup> field integral independent of the gap by their appropriate size and spacing to the end pole. Here, a different solution is proposed.

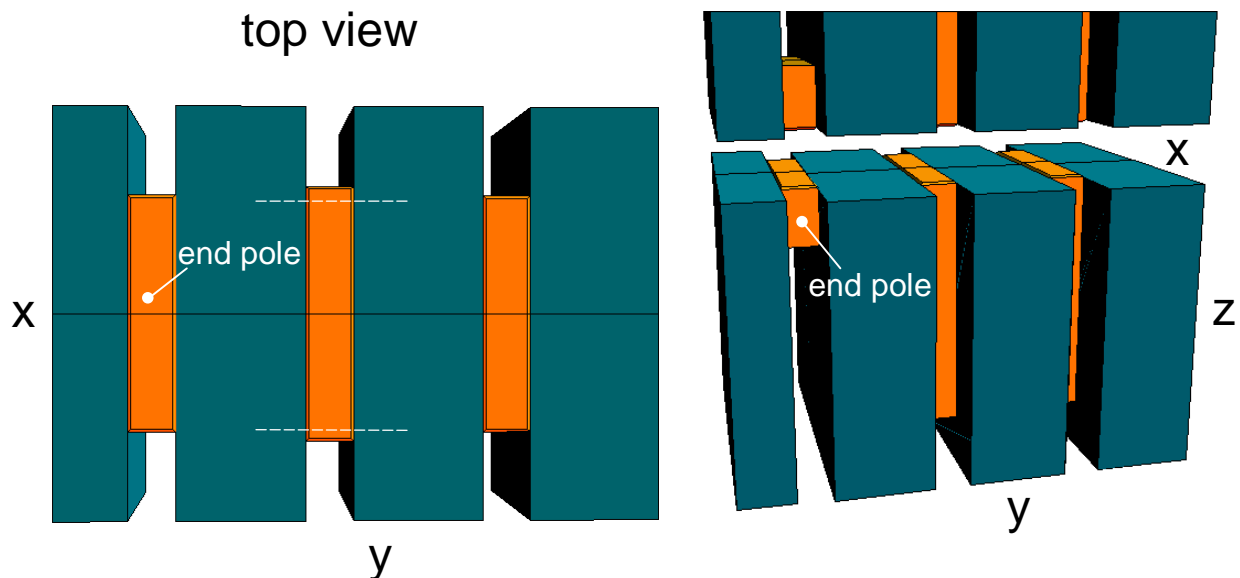


**Fig. 7:** End pole configuration; the length of the last magnet, the height of the last pole, and the width of the 2<sup>nd</sup> last pole are modified in order to adjust the field integrals to zero independent of the gap value.

For an unbalanced magnet structure, the gap dependence of the 1<sup>st</sup> field integral often exhibits a bump-like pattern with a sharp decline at the low gap side and a slow decay towards zero for large gaps where the magnetic field also approaches zero. The abrupt drop-off is due to the exponential increase of the peak field  $B_0$  with decreasing gap (Eq. 1) and complicates the field integral adjustment in the small gap range. The means to compensate this behavior should show the reverse gap dependence. Furthermore, the end pole configuration should be good-natured in terms of a stable and sufficiently large tuning range in order to also correct field errors due to the imperfect magnet and pole material. In this study the length of the last magnet, the height of the last pole as well as the width of the 2<sup>nd</sup> last pole are used to tune the 1<sup>st</sup> field integral. According to usual procedures for magnetic survey and shimming additionally the vertical position of the last magnet and pole can be varied. Figure 7 illustrates the geometry of the end pole design. This end pole arrangement comes close to a so-called “+1/4-3/4+1”-end field which, under ideal conditions, creates a true on-axis trajectory. Here, the trajectory is slightly shifted off-axis by a negligible amount as pointed out below.

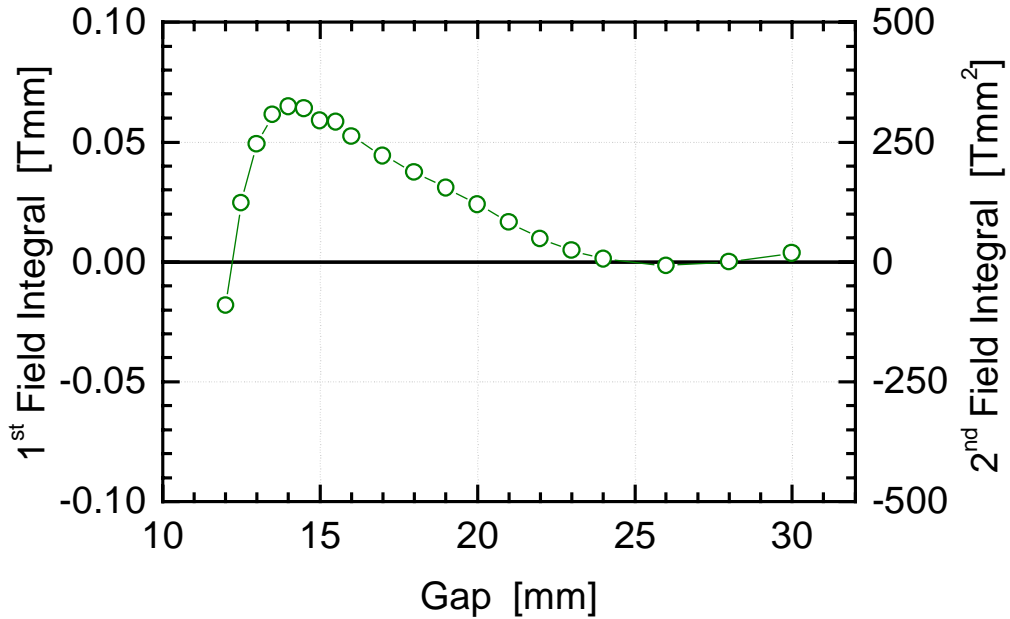


**Fig. 8:** Gap dependence of the magnetic field integrals. The 2<sup>nd</sup> field integral values are extrapolated to a 5 m long magnet structure.

The gap dependence of the 1<sup>st</sup> field integral has been studied separately for the different modified end pole parameters which all exhibit an individual signature. Multi-parameter calculations have been carried out to iteratively approach balanced field integrals for all relevant gap values. There is no unique solution for this problem but several configurations which trim the field integrals independent of the gap. However, some of them diverge quicker than others for tiny changes of certain parameters. The result of this optimization procedure is shown in Fig. 8. The gap dependence of the field integrals still exhibits the bump-like pattern but its size is reduced to a very small scale.

A maximum residual 1<sup>st</sup> field integral of  $I_1 \approx 0.005$  Tmm is achieved for large gaps, i.e. short photon wave lengths while at 13 mm gap a value of  $I_1 = 0.05$  Tmm remains. The corresponding values for the 2<sup>nd</sup> field integral are scaled to a 5 m long module and amount to  $I_2 \approx 25$  Tmm<sup>2</sup> and  $I_2 = 250$  Tmm<sup>2</sup>, respectively. This indicates that the specified maximum value for  $I_{1,2}$  is still exceeded in the medium gap range. Figure 8 reflects the present status of this design issue which requires further investigations. More sophisticated solutions in the end pole optimization including a modification of the pole shape will be elaborated in the future. Besides, the placement of shims which has not yet been included in the calculation can partly compensate the remaining gap dependence by two means, i.e. by flattening this curve and by shifting it vertically.

Fig. 9 displays the axial variation of the 1<sup>st</sup> and 2<sup>nd</sup> field integral for the open and closed gap position. The electron beam experiences a regular periodic excursion of about  $\pm 2.5$   $\mu\text{m}$  ( $\pm 1.2$   $\mu\text{m}$ ) for a gap of 12 mm (24 mm) with a mean off-axis trajectory displacement of

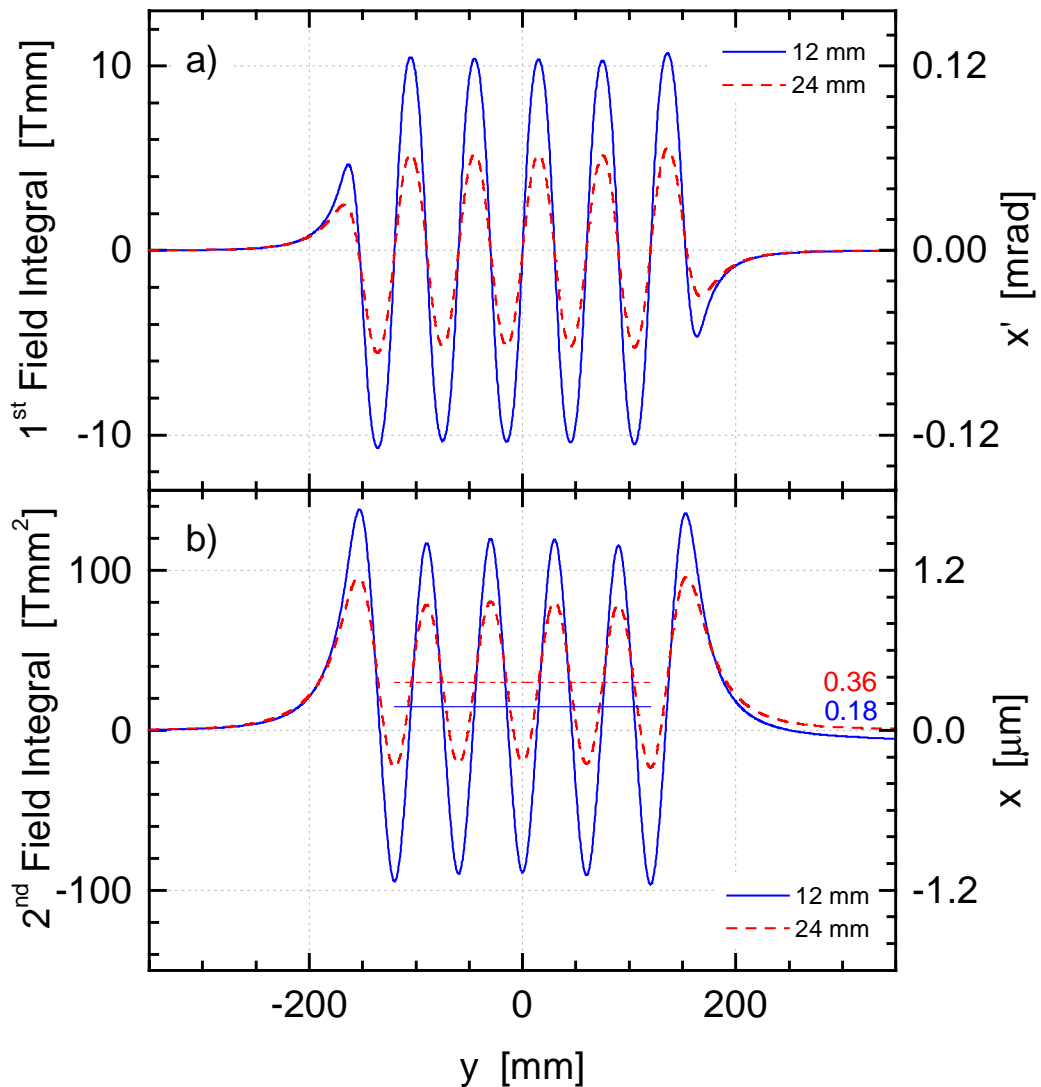


**Fig. 9:** a) 1<sup>st</sup> field integral along the undulator axis (five periods) for open and closed gap position. b) 2<sup>nd</sup> field integral corresponding to (a); the horizontal lines indicate the average trajectory in the magnet structure. The small gap dependent displacement is fully negligible as it is less than 1% of the rms transverse beam size.

$\sim 0.2 \mu\text{m}$  ( $\sim 0.4 \mu\text{m}$ ) which is fully negligible compared to the rms beam size of  $\sim 35 \mu\text{m}$ . In particular, this holds for the gap dependent relative shift of the trajectory.

Independent from a passive balancing of the field integrals which should be as capable as possible there could be varying time dependent conditions or thermal effects which necessitate active correctors like steering coils. The steerers are located in the intersections between two undulator segments; the horizontal corrector will be integrated within the phase shifter consisting of a three-magnet chicane [4] while a separate small coil serves to steer in the vertical direction. These correctors will be used to achieve the ultimate zero-adjustment of both field integrals. It is well established at many synchrotron storage rings to use active correctors, which are powered by gap dependent current settings. These values are frequently updated during dedicated diagnostic runs. The undulator control system [3] for TESLA will also be built in a modular way so that gap dependent current values can individually be set for each segment as a bias adjustment to which additional temporary kicks can be superimposed.

## 5 Radiation Damage

Radiation resistance is the major concern about long term stability of permanent magnet insertion devices. It has been pointed out in more detail in TDR, Sect. 4.3.2.3. [1] that the precautions foreseen for the TESLA FEL should be sufficient to allow the use of NdFeB magnet material.

In contrast to the undulator at the TESLA Test Facility (TTF), the XFEL undulators discussed here are gap variable devices which can be fully opened during the machine commissioning phase to avoid radiation damage to the magnet structures. A collimator system will confine the electron beam and scrape electrons which otherwise could hit the undulator due to either a missteered beam or dark current which is far outside the transverse and longitudinal phase space of the regular beam. The TTF undulator did up to now profit a lot from the collimator system installed there. A fast interlock system fed by various means of beam loss or radiation monitors will be an additional tool to prevent the magnet structures from radiation damage. A rough estimate has been made that NdFeB magnet material under worst case circumstances will have a lifetime of about 35 years before demagnetization exceeds 1%. Finally, a further step towards improved radiation resistance is the use of SmCo permanent magnets instead of NdFeB. This implies, however, two drawbacks, namely a reduced remanent magnetization in the order of  $\sim 10\%$  and secondly about 30% higher costs for the PM material which results in extra costs of about 45% for the magnet structures. Concerning the magnet design no general modifications are necessary in this case though the optimum dimensions for magnets and poles as well as the end pole configuration have to be recalculated as also the magnet volume needs to be increased to achieve the same peak field values.

## 6 Concluding Remarks

The magnet design proposed here is representative for all planar TESLA undulators. The dimensions of poles and magnets have been designed in a way that the peak field is maximized while all field requirements, e.g. regarding the transverse field roll-off, are fulfilled. A peak field of 1.33 T has been achieved with an amount of 400 cm<sup>3</sup> NdFeB magnet material per undulator period ( $\lambda_U = 60$  mm) for SASE1/4. The resulting geometrical dimensions are 8×40×55 mm<sup>3</sup> (L×W×H) and 22×70×65 mm<sup>3</sup> for poles and magnets, respectively. A compact end pole configuration has been found that de facto provides an on-axis trajectory and keeps the residual field integral close to zero independent of the magnetic gap.

A magnet design like the one presented here always considers ideal properties. In the real structure there occur of course field errors due different reasons: Inhomogeneity of the PM material, tolerances in the magnet and especially in the pole geometry, or alignment errors of the magnet stack within a structure all lead to small local field distortions, e.g. peak field fluctuations, which furthermore might add up to residual field integrals. As the field tolerances for an X-ray FEL undulator are rather small it is necessary to elaborate efficient methods to thwart these field errors by different means: The production process of the magnet material itself contains considerable potential for improvement of both statistical and systematic field errors [8]; several issues have been emphasized that deserve detailed investigation in an R&D program which has to be set up together with a magnet manufacturer. Besides, shims with a predictable signature have to be considered. This issue is, however, no topic of the present report but strongly coupled to magnetic survey procedures. During the later production phase, assembling and magnetic survey will be performed by a commercial manufacturer. Survey and tuning procedures for this purpose have to be established in the near future.

## 7 Acknowledgement

We would like to thank Vitaly Papadichev for valuable discussions on magnet design issues.

## References

- [1] TESLA Technical Design Report Part V, Eds.: G. Materlik, T. Tschentscher, DESY Report 2001-XX, Chapter 4 (2001)
- [2] “A Prototype Gap Separation System for the TESLA Undulator”, M. Rüter, J. Pflüger, TESLA-FEL 2000-07
- [3] “Ein SIMATIC basiertes Kontrollsystem für die Undulatoren des TESLA Röntgenlasers”, H.H. Radszuweit, J. Krunkowski, J. Pflüger, M. Tischer, TESLA-FEL 2000-09, in German
- [4] “A Prototype Phase Shifter for the Undulator Systems at the TESLA X-ray FEL”, J. Pflüger, M. Tischer, TESLA-FEL 2000-08
- [5] “Field Accuracy Requirements for the Undulator Systems of the X-ray FELs at TESLA”, B. Faatz, J. Pflüger, TESLA-FEL 2000-14
- [6] “Influence of Different Focussing Solutions for the TESLA X-ray FELs on Debunching of the Electron Beam”, B. Faatz, TESLA-FEL 2000-15
- [7] “Conceptual Design of a Planar Helical Undulator for the TESLA SASE FEL”, J. Bahrtdt, A. Gaupp, U. Englisch, W. Frentrup, M. Scheer, TESLA-FEL 2000-11
- [8] “Manufacturing Considerations of the Magnetic Structures for the Undulators for the XFEL at TESLA”, J. Pflüger, M. Tischer, F.J. Börgemann, R. Cremer, B. Schleede, TESLA-FEL 2000-10
- [9] “Conceptual Design of a 500 GeV  $e^+e^-$  Linear Collider with Integrated X-ray Laser Facility” (TESLA CDR), Eds.: R. Brinkmann, G. Materlik, J. Rossbach, A. Wagner, DESY 1997-048, Vol. II, Chapter 5 (1997)
- [10] “Design Considerations for a 1 Å SASE Undulator”, P. Elleaume, J. Chavanne, B. Faatz, Nucl. Instr. Meth. A 455, 503 (2000); TESLA-FEL 2000-16
- [11] “Physical and Optical Properties of Rare Earth Cobalt Magnets”, K. Halbach, Nucl. Instr. Meth. 187, 109 (1981); “Permanent Magnet Undulators”, K. Halbach, Journal de Physique, C 1 suppl. 2, 211 (1983)
- [12] TESLA Technical Design Report Part II, Eds.: R. Brinkmann et al., DESY Report 2001-XX, Sect. 9.7. (2001)  
TESLA Technical Design Report Part V, Eds.: G. Materlik, T. Tschentscher, DESY Report 2001-XX, Sect. 4.3.2.1. (2001)
- [13] “Computing 3D Magnetic Field from Insertion Devices”, P. Elleaume, O. Chubar, J. Chavanne, Proc. of the PAC, Vancouver, 3509 (1997); “A 3D Magnetostatics Computer Code for Insertion Devices”, O. Chubar, P. Elleaume, J. Chavanne, J. Synchr. Rad. 5, 481 (1998)